

# Light-Induced Protein Conformational Changes in the Photolysis of Octopus Rhodopsin

Masashi Nakagawa, Satoshi Kikkawa, Tatsuo Iwasa, and Motoyuki Tsuda

Department of Life Science, Himeji Institute of Technology, Harima Science Garden City, Kamigori, Akoh-gun, Hyogo 678-12, Japan

**ABSTRACT** Light-induced protein conformational changes in the photolysis of octopus rhodopsin were measured with a highly sensitive time-resolved transient UV absorption spectrophotometer with nanosecond time resolution. A negative band around 280 nm in the lumirhodopsin minus rhodopsin spectra suggests that alteration of the environment of some of the tryptophan residues has taken place before the formation of lumirhodopsin. A small recovery of the absorbance at 280 nm was observed in the transformation of lumirhodopsin to mesorhodopsin. Kinetic parameters suggest that major conformational changes have taken place in the transformation of mesorhodopsin to acid metarhodopsin. In this transformation, drastic changes of amplitude and a shift of a difference absorption band around 280 nm take place, which suggest that some of the tryptophan residues of rhodopsin become exposed to a hydrophilic environment.

## INTRODUCTION

Rhodopsin, an integral membrane protein consists of a chromophore, the 11-*cis* isomer of retinal, covalently bound via a protonated Schiff base to the  $\epsilon$ -amino group of a lysine residue of the apoprotein opsin. Light isomerizes the 11-*cis* chromophore to the all-*trans* form, resulting in protein conformational changes in rhodopsin that initiate the enzymatic cascade, resulting in the electrical excitation of the photoreceptor cell (Stryer, 1986; Tsuda, 1987). The light-induced protein conformational changes in the photochemical sequence of rhodopsin are of fundamental importance for understanding the visual process. Although the primary photochemistries of vertebrate and invertebrate rhodopsins are similar, vertebrate rhodopsins eventually hydrolyze to free retinal and opsin, whereas invertebrate ones reach a stable pigment, metarhodopsin. In octopus, rhodopsin absorbs maximally at 476 nm. Acid metarhodopsin, a stable photoproduct under physiological conditions, absorbs at 514 nm and photoregenerates to rhodopsin upon orange light illumination (Tsuda, 1987; Tsuda et al., 1989).

The photoreversibility of octopus rhodopsin enables us to apply several spectroscopic methods to elucidate the structure and function of its photochemical intermediates: low-temperature (Tsuda et al., 1980) and time-resolved absorption spectroscopy (Tsuda, 1979; Ohtani et al., 1988; Taiji et al., 1992), resonance Raman spectroscopy (Kitagawa and Tsuda, 1980; Pande et al., 1984, 1987), and low-temperature and time-resolved Fourier transform infrared spectroscopy

(Bagley et al., 1989; Masuda et al., 1993a,b). These results showed that the primary photoproduct, primerhodopsin ( $\lambda_{\max}$ : 580 nm), forms within 400 fs (Taiji et al., 1992) and is transformed to bathorhodopsin ( $\lambda_{\max}$ : 540 nm) after 50 ps (Ohtani et al., 1988). Bathorhodopsin converts to lumirhodopsin, mesorhodopsin, and finally, acid metarhodopsin (Tsuda, 1979).

Although the chromophore absorption spectra in the photochemical intermediate sequence upon irradiating octopus rhodopsin have been studied in detail, the protein conformational changes of these transformations are poorly understood. The enthalpy changes associated with each of the major steps in the phototransformation of octopus rhodopsin have been measured by direct photocalorimetry (Cooper et al., 1986). Formation of bathorhodopsin at very low temperature involves an energy uptake of about 130 kJ/mol, corresponding to storage of over 50% of the absorbed photon's energy. This energy is dissipated at stepwise protein conformational changes in the subsequent intermediates to give a final photoproduct (acid metarhodopsin) at a level comparable to the amount of the initial rhodopsin. Protein conformational changes between rhodopsin and acid metarhodopsin were observed in spin label (Kusumi et al., 1980) and Fourier transform infrared (Masuda et al., 1993a, b) studies, but these methods were not able to detect any short-lived intermediates.

Upon perturbation, absorption changes in proteins at  $\sim 280$  nm are interpreted as arising from alteration of the environment of their aromatic amino acids. Thus protein conformational changes in the photolysis of octopus rhodopsin are expected to be reflected by UV absorbance changes, although the changes are likely to be very small.

In this work, we developed a sensitive absorption spectrophotometer with nanosecond time resolution to measure small changes in the UV absorbance and used it to successfully measure protein conformation changes associated with the photolysis of octopus rhodopsin.

Received for publication 15 October 1996 and in final form 28 January 1997.

Address reprint requests to Dr. Motoyuki Tsuda, Department of Life Science, Himeji Institute of Technology, Harima Science Garden City, Kamigori, Akoh-gun, Hyogo 678-12, Japan. Tel.: -81-7915-8-0196; Fax: -81-7915-8-0197; E-mail: mtsuda@sci.himeji-tech.ac.jp.

© 1997 by the Biophysical Society

0006-3495/97/05/2320/09 \$2.00

## MATERIALS AND METHODS

### Preparation of octopus rhodopsin

Microvillar membranes of octopus photoreceptors were prepared from the eyes of *Paraoctopus defleini* as previously described (Tsuda et al., 1986). After isolation by sucrose flotation, the microvillar membranes were repeatedly washed with buffer A (400 mM KCl, 10 mM MgCl<sub>2</sub>, 10 mM 2-(*N*-morpholino)ethanesulfonic acid (pH 6.5), 1 mM dithiothreitol (DTT), 1 mM benzamidine-HCl, 20 μM 4-(amidinophenyl)methanesulfonyl fluoride (APMSF)) and then with buffer B (10 mM 2-(*N*-morpholino)ethanesulfonic acid (pH 6.5), 1 mM DTT, 1 mM benzamidine-HCl, 20 μM APMSF). Upon ultracentrifugation, the resulting pellets gave two distinct layers. The fluffy layer was pooled, and the rhodopsin was solubilized in 10 mM Tris-HCl buffer (pH 7.4) containing 1 mM DTT, 1 mM benzamidine-HCl, 20 μM APMSF, and 1% (w/v) sucrose monolaurate and then centrifuged at 240,000 × *g* for 1 h. Further purification of the octopus rhodopsin was carried out by affinity chromatography using Con-A Sepharose (Pharmacia Biotech, Uppsala, Sweden). The solubilized rhodopsin was applied to a Con-A column that had previously been equilibrated with a solution containing 10 mM Tris-HCl (pH 7.4), 0.5 M NaCl, 1 mM CaCl<sub>2</sub>, 1 mM MnCl<sub>2</sub>, and 0.1% sucrose monolaurate. The same buffer solution was used to wash the column thoroughly. Subsequently, the rhodopsin was eluted from the column with 250 mM α-methyl-D-mannopyranoside in the equilibrating buffer solution. The fractions that had absorption ratios ( $A_{280}/A_{476}$ ) of less than 4.0 were collected and dialyzed with a solution containing 10 mM 3-(*N*-morpholino)propanesulfonic acid (pH 7.4) and 0.2% sucrose monolaurate to remove the α-methyl-D-mannopyranoside.

An important property of sucrose monolaurate that facilitated this work is its low absorbance in the UV and its low fluorescence on excitation. Moreover, it is expected that conformation of octopus rhodopsin in sucrose monolaurate is close to that in the microvillar membranes, because the lifetime of the photo intermediates (Kusumi et al., 1983) and pK<sub>a</sub> of the acid- to alkaline-metarhodopsin transition (Liang et al., 1994) in sucrose monolaurate are close to the values observed in the microvillar membranes.

### Spectroscopic measurements

The absorption spectra were recorded with a Shimadzu MPS2000 spectrophotometer equipped with a cross-illumination attachment. The fluorescence spectra were recorded with a Shimadzu RF5000 fluorometer. Low-excitation light intensities were used throughout to reduce the photolysis of the rhodopsin. Slit settings for the fluorometer were 3.0 nm for the excitation and 5.0 nm for the emission measurements. No detectable photobleaching of the rhodopsin sample was observed under these conditions.

### Nanosecond spectroscopy

The actinic light source used for the nanosecond flash photolysis studies was a Nd-YAG laser (1.064 μm with a 8-ns pulse width (FWHM) pulse, model NY 60; Continuum, Santa Clara, CA). Excitation of the sample was achieved using the amplitude spontaneous emission (ASE) (460 nm wavelength) generated by passing the third harmonic of the Nd-YAG laser (355 nm) into coumarin 460 (Exiton, Dayton, OH) in ethanol. The excitation pulse energy was approximately 8 mJ. The probe light source was a continuous Xe lamp (model L2195; Hamamatsu, Iwata, Japan) to allow absorption measurements over a wide range of wavelengths (240–700 nm). The excitation pulse and monochromatic probe beam were focused onto the sample cell at right angles (6 mm × 10 mm section with a 10-mm path length). The probe light was detected by a photomultiplier after passing through a second monochromator. The sample was contained in a closed system whereby fresh sample was pumped into the irradiated area of a quartz cuvette after each pulse. Downstream from the probe beam, the photolyzed sample was irradiated with orange light transmitted through a cutoff filter (λ > 580 nm, Toshiba, O-58) to convert any acid metarhodopsin that had been formed back to rhodopsin. The absorbance of the samples for experiments in the visible range was 0.39 at 476 nm, and for

the UV range experiments it was 0.79 at 280 nm (0.19 at 476 nm). The sample temperature in the flow system was maintained at 15°C with a thermal bath RMS6 (Lauda, Lauda-Königshofen, Germany).

## RESULTS

### UV and visible absorption spectral changes between rhodopsin and acid metarhodopsin

Fig. 1 *A* shows the absorption spectrum of octopus rhodopsin (*curve 1*). The absorption maxima of the chromophore and the protein are located at 476 and 280 nm, respectively. When the rhodopsin solution was irradiated with 440 nm light (V44 Toshiba) for 1 min, the chromophore absorption maximum shifted to longer wavelengths by 30 nm, and the absorbance at wavelengths of >470 nm increased and the absorbance at 279 nm decreased (*curve 2* in Fig. 1). The difference spectrum (Fig. 1 *B*) between irradiated rhodopsin and rhodopsin has a positive band at 530 nm, showing the formation of acid metarhodopsin, and a negative band corresponding to the depletion of the original pigment. The transformation of rhodopsin to acid metarhodopsin also results in absorption changes at the UV range. These are characterized by a large decrease in bands near 234 nm and around 287 nm, the latter having fine structure. These bands are attributed to the alteration of the environment of aromatic acid residues such as tryptophan or tyrosine.

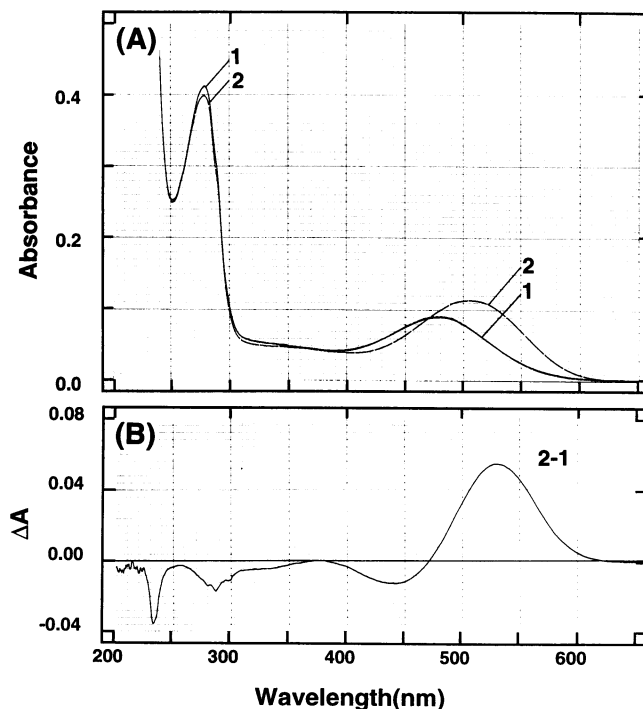


FIGURE 1 (A) Absorption spectra in the photochemical interconversion among rhodopsin and acid metarhodopsin in sucrose monolaurate. Rhodopsin at pH 6.5 (*curve 1*) was irradiated with blue light for 1 min. (B, *curve 2*) Difference absorption spectrum between irradiated rhodopsin (*curve 2* in A) and rhodopsin (*curve 1* in A)

### Fluorescence spectral changes in converting from rhodopsin to acid metarhodopsin

Fig. 2 A shows the fluorescence spectra of rhodopsin (*curve 1*) and metarhodopsin (*curve 2*) excited at 280 nm. The intensity of fluorescence emission at 330 nm increased when rhodopsin was converted to acid metarhodopsin. When metarhodopsin was illuminated with orange light to regenerate rhodopsin, the intensity of the fluorescence band at 330 nm returned to the original level. Fig. 2 C shows the excitation spectra of rhodopsin and metarhodopsin while the 330-nm fluorescence emission is monitored. These excitation spectra are also photoreversible upon illumination with blue and orange light. The difference excitation spectrum between rhodopsin and acid metarhodopsin was characterized by a sharp band near 239 nm and a second one with fine structure centered at 283 nm, which is essentially the same as the difference UV absorption spectrum between rhodopsin and acid metarhodopsin shown in Fig. 1 B. These results prompted us to study the dynamics of the protein conformational changes in the photochemical sequence of octopus rhodopsin using UV absorbance changes.

### Three-dimensional spectral changes in the photolysis of octopus rhodopsin

Transient chromophore absorption spectra of the photochemical intermediates of octopus rhodopsin using time-resolved spectroscopy were previously reported (Tsuda, 1979). In these transformations, the chromophore absorp-

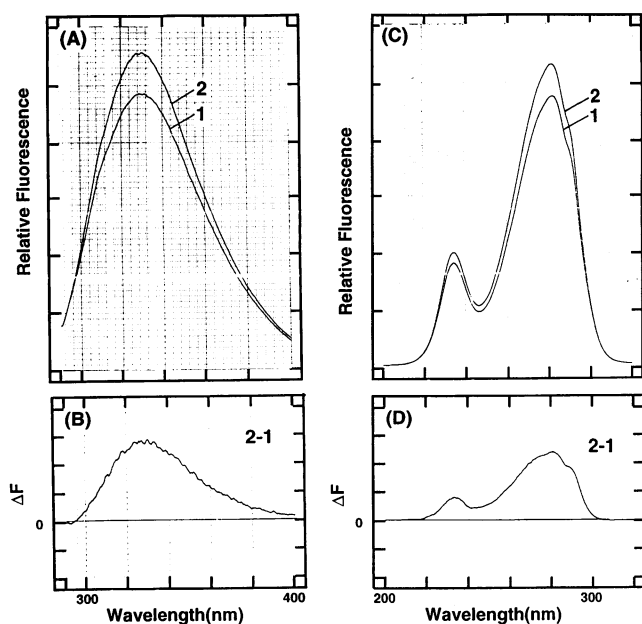


FIGURE 2 (A) Fluorescence emission spectra of octopus rhodopsin (*curve 1*) and irradiated rhodopsin (*curve 2*) excited at 280 nm. (B) Difference fluorescence emission spectrum between curve 2 and curve 1 in A. (C) Fluorescence excitation spectra of octopus rhodopsin (*curve 1*) and irradiated rhodopsin monitoring 330 nm fluorescence emission. (D) Difference fluorescence excitation spectrum between curve 2 and curve 1 in C.

tion changes located in the visible range are large enough to be routinely measured by a conventional flash-photolysis apparatus. On the other hand, it is hard to measure the time-resolved absorption changes of the intermediates in the UV. This is primarily because the absorption changes taking place are very small and the protein's absorbance is high. Moreover, the intensity of the standard UV light source is weak and the sensitivity of most of the photo detectors in the UV range is low. Hence we sought to develop a highly sensitive spectrophotometer with nanosecond time resolution to measure small changes in absorbance in the UV range.

In this study, the time course of the absorption changes at fixed wavelength versus time was measured using a photomultiplier. This is the method of choice in measuring minute changes to give more accurate and reliable results. To get a good signal-to-noise ratio, it was necessary to record more than 1024 traces at each 5-nm wavelength interval. The immense number of measurements taken would not have been possible were it not for the photoreversibility of octopus rhodopsin.

Fig. 3 shows the three-dimensional transient difference spectra between photointermediates and rhodopsin. The time course ( $-40$  to  $160 \mu\text{s}$ ) of flash-induced transient difference spectra of the intermediates at the visible wavelength range (350–600 nm, Fig. 3 A) and at the UV range (260–350 nm, Fig. 3 B) are presented. After the flash (the first data point obtained is after a  $0.16\text{-}\mu\text{s}$  time delay), the transient difference spectra in the visible show a positive band at 540 nm and a negative band at 450 nm. The amplitude decreases within a few microseconds and then increases again to reach a plateau after  $160 \mu\text{s}$ . On the other hand, the transient difference spectra in the UV in Fig. 3 B show that a negative band around 280 nm appears after the flash, which broadens and intensifies at longer delay times. It should be pointed out that, whereas in the visible region (Fig. 3 A) the maximum absorbance change measured was about 0.06, in the UV region it is only 0.006.

### Time-resolved difference spectral changes

To effectively interpret our data so as to correlate the chromophore and protein absorption changes during the photolysis of rhodopsin, it is necessary to slice the 3-D spectra shown in Fig. 3 along the time axis to generate time-resolved difference spectra (as those shown in Figs. 4 and 5) and along the wavelength axis to generate the time course of absorption changes (Figs. 6 and 7). Fig. 4 A shows the time-resolved difference visible spectra (chromophore spectral region) obtained after photolysis of octopus rhodopsin at delay times from  $0.32 \mu\text{s}$  to  $2.56 \mu\text{s}$ . At the  $0.32\text{-}\mu\text{s}$  time delay (*curve 1* in Fig. 4 A), there is an increase in absorbance at 540 nm (corresponding to the formation of mesorhodopsin) concomitant with a decrease at 450 nm (corresponding to the depletion of the original pigment). At delay times from  $0.64 \mu\text{s}$  to  $2.56 \mu\text{s}$ , however, the band at

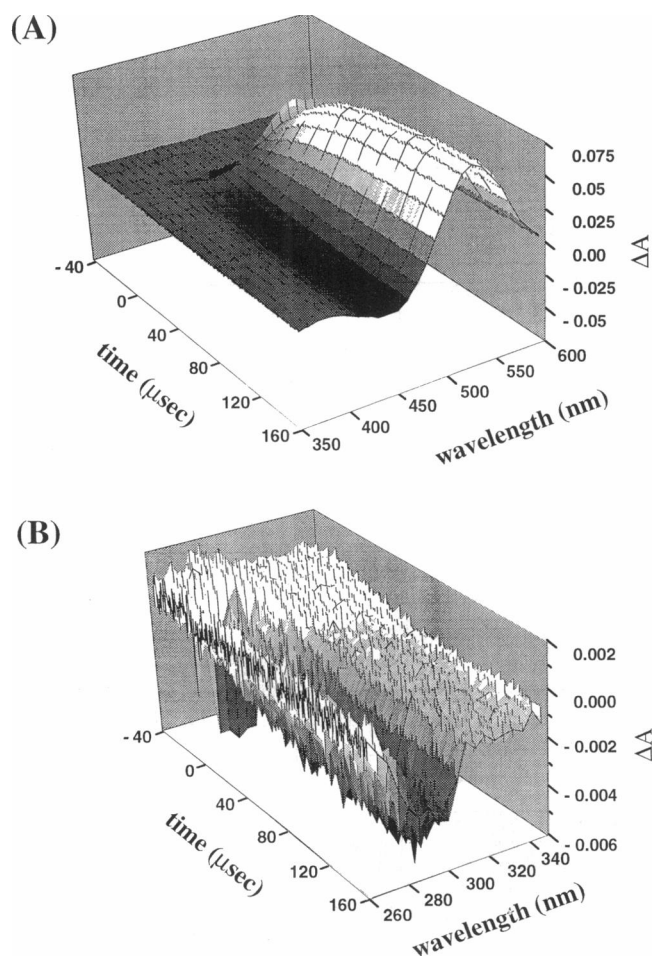


FIGURE 3 Three-dimensional time-resolved difference spectra of octopus rhodopsin after a blue flash. (A) Visible range (350–600 nm) and (B) UV range (260–350 nm).

540 nm fell and the band at 450 nm partially recovered, with an isosbestic point at 490 nm (Process 1). In the next 102  $\mu$ s, as shown in Fig. 4 B, the band at 530 nm rose and the band at 460 nm fell with an isosbestic point at 470 nm (Process 2). There was no further change in the difference spectra obtained after 102  $\mu$ s. Furthermore, the difference spectrum at 102  $\mu$ s (curve 9 in Fig. 4) was identical to the difference spectrum of rhodopsin and the final photoproduct, acid metarhodopsin, shown in Fig. 1 B. These results imply that there are intermediates that are precursors to acid metarhodopsin.

In a previous paper (Tsuda, 1979) we presented transient absorption spectra of the intermediates in the photochemical sequence of octopus rhodopsin by a flash photolysis-rapid scan spectroscopy. Transient spectra in the photolysis of rhodopsin in digitonin showed that after a delay time of 100 ms, the absorption bands began to shift toward longer wavelengths and the curves passed through an isosbestic point at 480 nm, with a concomitant increase in absorbance at 520 nm and a decrease in absorbance at 460 nm. These spectral

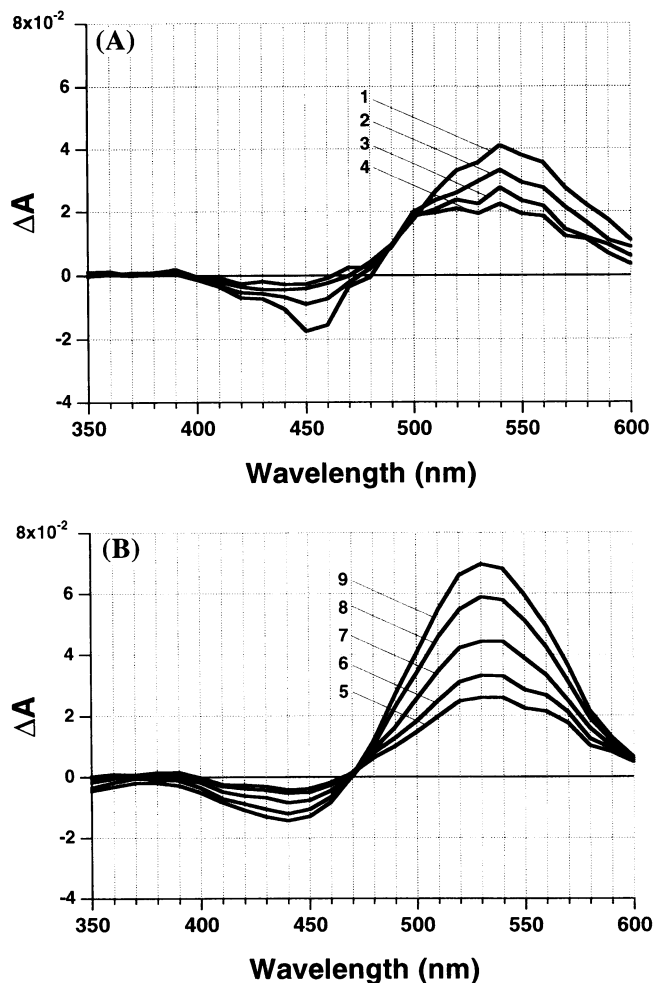


FIGURE 4 Time-resolved difference absorption spectra of octopus rhodopsin in the visible range (350–600 nm). (A) Time after excitation; 1, 0.32  $\mu$ s; 2, 0.64  $\mu$ s; 3, 1.28  $\mu$ s; 4, 2.56  $\mu$ s. (B) Time after excitation; 5, 6.4  $\mu$ s; 6, 12.8  $\mu$ s; 7, 25.6  $\mu$ s; 8, 51.2  $\mu$ s; 9, 102  $\mu$ s.

changes are essentially the same as those of Process 2 in the present work, although the rate is retarded by the use of digitonin (Kusumi et al., 1983). Hence we assign Process 2 as the transformation from mesorhodopsin to acid metarhodopsin. Because the precursor of mesorhodopsin is lumirhodopsin (based on previous results obtained by low-temperature spectroscopy; Tokunaga et al., 1975), Process 1 is assigned to the transformation of lumirhodopsin to mesorhodopsin.

Fig. 5 shows the time-resolved difference UV spectra (protein spectral region) at 0.8  $\mu$ s (curve 1) to 102  $\mu$ s (curve 6) after the photolysis of octopus rhodopsin. At short delay times (0.8  $\mu$ s), the absorbance at 280 nm decreased. Up to the next 102  $\mu$ s (curve 6), a gradual shift toward longer wavelengths was observed. Additionally, there was broadening and an increase in band intensity. It is to be noted that these protein spectral changes accompanied those shown in Fig. 4 B, in the visible range, which were assigned to the transformation of mesorhodopsin to acid metarhodopsin.

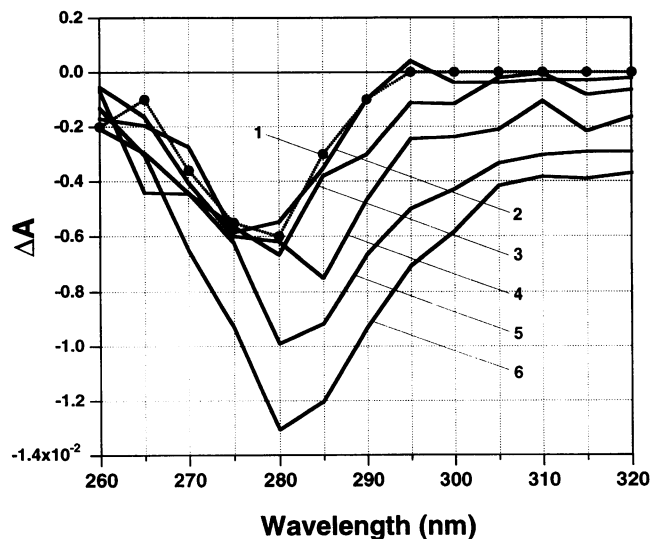


FIGURE 5 Time-resolved difference absorption spectra of octopus rhodopsin in the UV range (260–320 nm) after a blue flash. The amplitude of curve 1 was taken in the same way that the time course in Fig. 6 was extrapolated to time 0. Time after excitation: 2, 6.4  $\mu$ s; 3, 12.8  $\mu$ s; 4, 25.6  $\mu$ s; 5, 51.2  $\mu$ s; 6, 102  $\mu$ s.

We failed to get the time-resolved difference UV spectra between 0.32  $\mu$ s and 5.12  $\mu$ s corresponding to the transformation of lumirhodopsin to mesorhodopsin. Although more than 1024 traces for each wavelength were accumulated to improve the signal-to-noise ratio, the time courses for absorption changes at 280 nm and 290 nm as shown in Fig. 6 were too noisy to generate reliable time-resolved difference spectra.

### Time course of absorbance changes in the transformation of the intermediates

Fig. 6, A and B, shows the time course of flash-induced absorption changes of octopus rhodopsin at 530 nm and 420 nm. An abrupt increase in absorbance at 530 nm upon flash excitation indicates the formation of lumirhodopsin, whereas the decrease in absorbance at 420 nm implies the depletion of the original pigment. Within 4  $\mu$ s, there is a noticeable decrease in absorbance at 530 nm, with a concomitant increase in absorbance at 420 nm. These features characterize the chromophore absorption changes from lumirhodopsin to mesorhodopsin. After 4  $\mu$ s, the absorbance at 530 nm increased while the absorbance at 420 nm decreased, corresponding to the absorbance changes observed at the same wavelength at slower scan times shown in Fig. 7, A and B.

Fig. 6, C and D, shows the time course of transient absorption changes at 290 nm and 280 nm. Upon flash excitation, the observed abrupt decrease in absorbance at 280 nm is attributed mainly to changes in the protein conformation as it undergoes transformation to lumirhodopsin. Within 4  $\mu$ s the absorbance at 280 nm increases. At longer times, however, there is a decrease in the trend, as con-

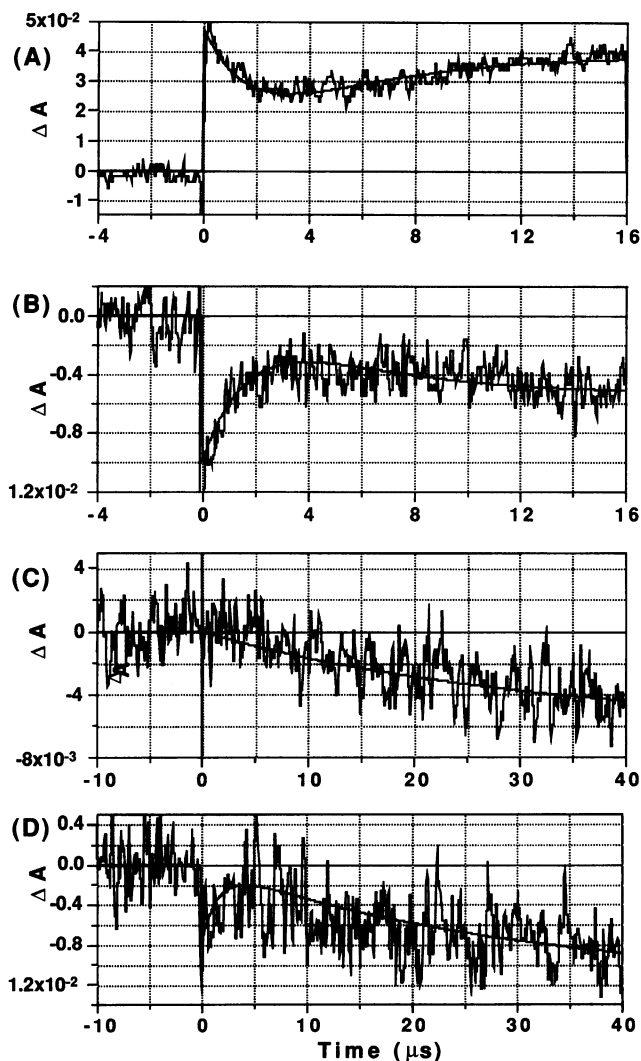


FIGURE 6 Time course of light-induced absorbance changes in octopus rhodopsin at a given wavelength. Absorbance changes at 530 nm (A), 420 nm (B), 290 nm (C), and 280 nm (D). Smooth curves represent the fitting curves with time constants  $\tau_1 = 1.5 \mu$ s,  $\tau_2 = 31 \mu$ s.

firmed by the slower scan time in Fig. 7 D. The absorption changes at 290 nm at early times are different from those at 280 nm. There are no absorbance changes during the first 5- $\mu$ s delay after flash excitation. However, at the later times, the absorbance decreased with time, giving a time profile that is essentially the same as that at 280 nm. These time courses in Fig. 7, C and D, in conjunction with the time-resolved difference spectra in Fig. 4, suggest that the sharp absorption band located around 280 nm characterizes the formation of lumirhodopsin, and the subsequent slight decrease in amplitude of the absorption band results from the transformation of lumirhodopsin to mesorhodopsin. The transformation of mesorhodopsin to acid metarhodopsin is characterized by a red shift of the broad absorption band around 280 nm with enhanced amplitude.

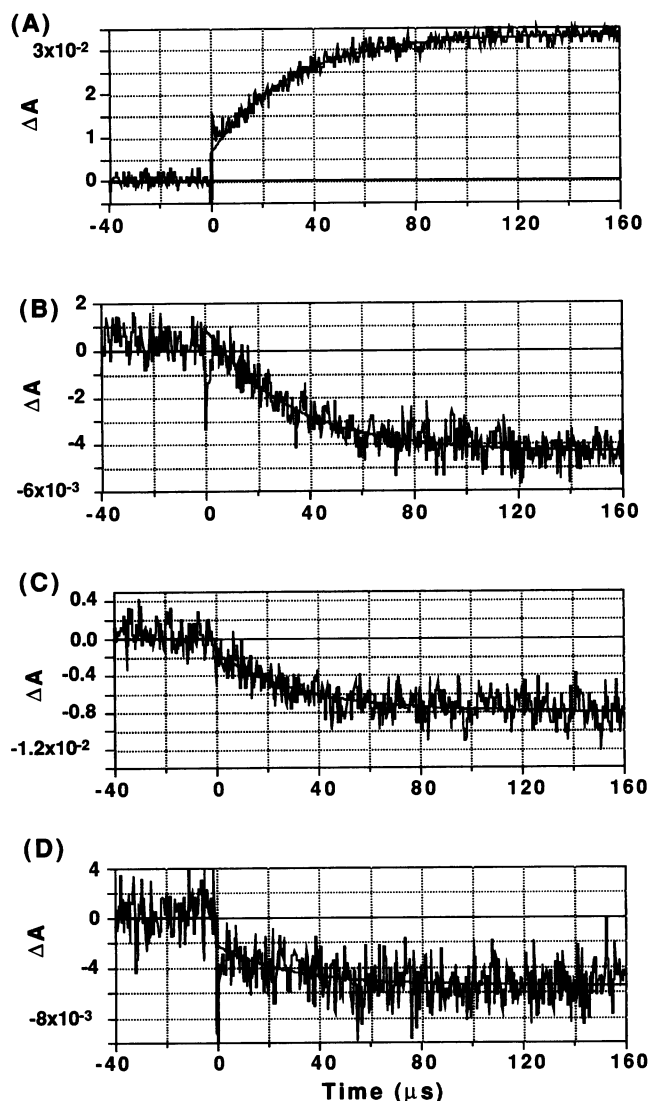


FIGURE 7 Time course of light-induced absorbance changes of octopus rhodopsin at a given wavelength. Absorbance changes at 530 nm (A), 420 nm (B), 290 nm (C), and 280 nm (D). Smooth curves represent the fitting curves with time constants of  $\tau_2 = 31 \mu\text{s}$ .

### Kinetic parameters

The detailed kinetic parameters for the transformations of the photointermediates were derived from the time courses obtained from both the chromophore and protein absorption bands shown in Figs. 6 and 7. The least-squares fitting analysis for the time courses in Fig. 7, A and B, gave  $31.0 \pm 0.7 \mu\text{s}$  as the time constant for the chromophore transformation from mesorhodopsin to acid metarhodopsin. The time constant for the chromophore transformation from lumirhodopsin to mesorhodopsin at a given temperature was derived from the time courses in Fig. 6, A and B. Because the slower part of the time course originated from the transformation of mesorhodopsin to acid metarhodopsin, the least-squares fitting analysis was done after subtracting the time constant of  $31.0 \pm 0.7 \mu\text{s}$  corresponding to the transformation of mesorhodopsin to acid metarhodopsin.

It is interesting to compare the time constants derived from protein absorption changes to those from chromophore absorption changes. The time constant for the conformational changes of the protein portion was estimated from the UV absorbance changes at 280 nm and 290 nm (Figs. 6 and 7). These were estimated by least-squares fitting to be  $33.6 \pm$  standard deviation  $\mu\text{s}$  and  $34.0 \pm 2.0 \mu\text{s}$ , respectively, which are slightly larger than those estimated from chromophore absorbance changes in the visible region.

To study the correlation between the rate of the protein conformational changes and the chromophore absorption changes, the rate constants for the absorption changes at 530 nm and 280 nm were examined at different temperatures from  $5^\circ\text{C}$  to  $25^\circ\text{C}$ . Fig. 8 shows an Arrhenius plot of the rate constants for the transformation of mesorhodopsin to acid metarhodopsin derived from absorbance changes monitored at 530 nm (closed circles) and 280 nm (open circles). The data points suggest that there is no significant difference between them. Temperature dependency of the rate constant for the transformation from lumirhodopsin to mesorhodopsin was also plotted in Fig. 8. Because the time course of absorbance changes at 280 nm was too noisy (as shown in Fig. 5) to derive reliable rate constants, only those based on absorption changes at 530 nm (closed square) were plotted. Kinetic parameters calculated according to the transition state theory are shown in Table 1. Because the activation enthalpy and entropy for the transformation of mesorhodopsin to metarhodopsin are larger than those for the transfor-

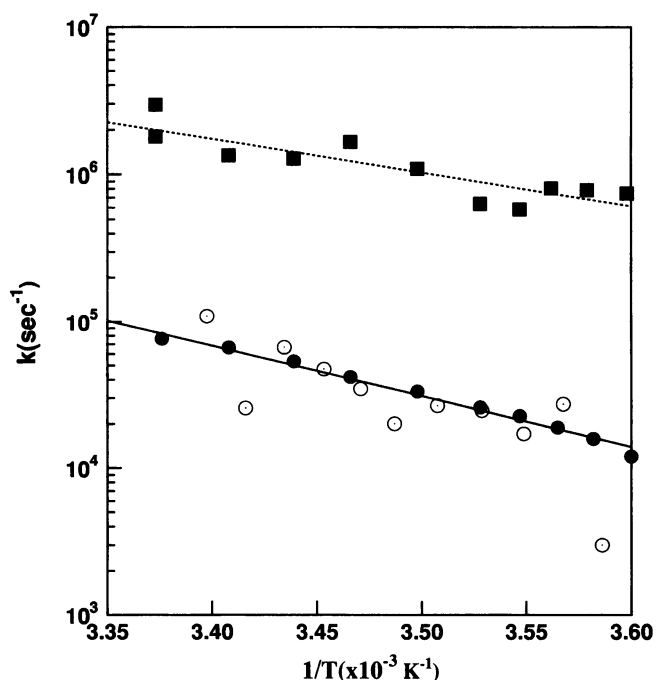


FIGURE 8 Arrhenius plot of the rate constants for two transformations processes. Closed squares represent the rate constant for the transformation of lumi- to mesorhodopsin observed at 530 nm. Closed circles and open circles represent the rate constant for that of meso- to metarhodopsin, which was obtained from absorbance changes at 530 nm and 280 nm, respectively. Straight lines were obtained by least-squares fitting.

**TABLE 1** Kinetic parameters for the formation of mesorhodopsin and acid metarhodopsin

Transformation	$E_a$ (kcal · mol <sup>-1</sup> )*	$\Delta G^\ddagger$ (kcal · mol <sup>-1</sup> ) <sup>#</sup>	$\Delta H^\ddagger$ (kcal · mol <sup>-1</sup> ) <sup>§</sup>	$\Delta S^\ddagger$ (kcal · mol <sup>-1</sup> K <sup>-1</sup> ) <sup>¶</sup>
Lumi → Meso	10.3	8.82	9.78	3.32
Meso → Meta	15.7	10.8	15.1	15.2

\*Activation energy.

<sup>#</sup>Free energy of activation.<sup>§</sup>Enthalpy of activation.<sup>¶</sup>Entropy of activation.

mation of lumirhodopsin to mesorhodopsin, major protein conformational changes in the photochemical sequence of octopus rhodopsin must have taken place during the transformation of mesorhodopsin to acid metarhodopsin.

## DISCUSSION

We have successfully measured protein conformational changes as well as chromophore absorption changes in the transformation of lumirhodopsin to mesorhodopsin and mesorhodopsin to metarhodopsin upon the photolysis of octopus rhodopsin.

### Absorption changes between rhodopsin and acid metarhodopsin

Illumination of octopus rhodopsin results in the formation of acid metarhodopsin, which is a stable photoproduct at physiological temperatures. Acid metarhodopsin converts to rhodopsin upon orange light illumination. The difference absorption spectrum between rhodopsin and acid metarhodopsin (Fig. 1 *B*) has a negative band at 438 nm and a positive band at 530 nm in the visible range. In addition, an intense negative band near 234 nm and a second band at 287 nm were observed in the UV range. Visible spectral changes of rhodopsin are due to the chromophore as influenced by the protein moiety. One interpretation of these UV difference spectral changes is that they originate from a second absorption band of the chromophore, because 11-*cis* retinal has a *cis* peak, whereas all-*trans* retinal lacks this second band (Sperling, 1973). However, the maximum wavelength of the *cis* peak located at 250 nm and its band shape are different from the difference spectrum in Fig. 1 *B*, which has fine structure. Alternatively, the UV difference spectrum is interpreted as being due to alterations of the environment of several aromatic amino acid residues such as tryptophan and tyrosine. As shown in previous studies (Guzzo and Pool, 1968, 1969; Ebrey, 1971), the quantum yield of fluorescence of the chromophore in opsin is very low. However, fluorescence emission from the aromatic acids of opsin is rather strong (Ebrey, 1972; Farrens and Khorana, 1995). The emission maximum of octopus rhodopsin and acid metarhodopsin is 330 nm when excited with 280-nm light, which is essentially similar to that of bovine rhodopsin (Ebrey, 1972). Tryptophan and tyrosine residues are the principal fluorescent amino acids in opsin, as they

are in all proteins that contain those aromatic amino acids. We studied the contribution of tyrosine as well as tryptophan to the fluorescence emission spectrum of octopus rhodopsin and acid metarhodopsin and concluded that the contribution of tyrosine to the whole fluorescence spectrum is less than 10% (Nakagawa et al., manuscript in preparation). These results are consistent with a UV resonance Raman study which shows that the tryptophan band at 1615 cm<sup>-1</sup> decreases, but no changes were found at 1601 cm<sup>-1</sup>, which would be expected if there were protonation of tyrosine residues in going from rhodopsin to acid metarhodopsin (Hashimoto et al., 1996). Moreover, the difference excitation spectrum between rhodopsin and acid metarhodopsin in Fig. 2 *B* is similar to the difference absorption spectrum between rhodopsin and acid metarhodopsin in Fig. 1 *A*. These results strongly suggest that the principal amino acid whose environment is altered in the transformation of rhodopsin to acid metarhodopsin is tryptophan.

After the transformation of rhodopsin to acid metarhodopsin, there is a small decrease in the fluorescence emission intensity (Fig. 2). At present it is unclear how much of the decrease in the fluorescence yield is due to an increase in energy transfer to the chromophore and how much is due to direct environment influences on the tryptophans. However, difference absorption changes between rhodopsin and acid metarhodopsin can be assigned based solely on alteration of the environment of the tryptophan. For this reason, we studied the protein conformational changes in the photolysis of octopus rhodopsin by measuring absorption changes around 280 nm.

### Transient conformational changes in the lumirhodopsin to acid metarhodopsin transition

The primary photoevent in rhodopsin is *cis-trans* isomerization of retinal, followed by the alteration in retinal-opsin interactions in discrete steps, which are identified as the intermediates with different absorption maxima. In addition to the visible absorption changes, protein conformational changes in these transformation were studied by absorption changes around 280 nm, which revealed the environment changes of tryptophan.

The first intermediate observed in the present work was lumirhodopsin. The difference absorption spectrum between lumirhodopsin and rhodopsin (*curve* 1 of Fig. 5) has a negative band whose absorption maximum is located at

280 nm. These results suggest that alterations in the environment of some of the tryptophan residues have taken place before formation of lumirhodopsin. At the 6.4- $\mu$ s time delay, lumirhodopsin is transformed to mesorhodopsin, where the absorbance at 280 nm recovered quite a bit. The amplitude of the absorbance changes at 280 nm in the transformation of lumirhodopsin to mesorhodopsin is one-half of those in the transformation from rhodopsin to lumirhodopsin. (Fig. 5). These results suggest that apparent environment changes around tryptophan in the transformation of lumirhodopsin to mesorhodopsin is small.

At delay times from 6.4  $\mu$ s to 102  $\mu$ s, the amplitude of the time-resolved difference spectra around 280 nm increased and the spectrum shifted toward longer wavelengths in the transformation of mesorhodopsin to acid metarhodopsin (Fig. 5). The absorption spectrum of tryptophan is sensitive to the polarity of the environment. In nonpolar media the spectrum shifts to longer wavelengths (Donovan, 1969). The decrease in amplitude and the shift of the absorption maximum around 280 nm to longer wavelengths accompany the change from mesorhodopsin to acid metarhodopsin (Fig. 5) and suggest that some tryptophan residues in rhodopsin move to a more polar environment. If these tryptophan residues are far from the chromophore, it is expected that the rate of chromophore absorbance changes could be different from that of tryptophan absorbance changes. We measured that temperature dependence of the rate of the chromophore absorption changes at 530 nm and the tryptophan absorption changes at 280 nm and concluded that these two rates are the same within error. These results suggest that the tryptophans that are changing are close to the chromophore.

Octopus rhodopsin contains 11 tryptophan residues, five of which are presumably in the membrane-embedded domain predicted from the primary structure of octopus rhodopsin (Ovchinnikov et al., 1988). There are four tryptophans (W161, W163, W167, W175) in the fourth helix, two of which are the counterparts of W161 and W175 of bovine rhodopsin. Tryptophan (W275) in the sixth helix of octopus rhodopsin corresponds to W265 of bovine rhodopsin. The maximum wavelengths of the chromophore absorption bands of the early intermediates (primerhodopsin, bathorhodopsin, hypsorhodopsin, lumirhodopsin) of bovine and octopus are similar to each other. If the chromophore absorption is sensitive to the perturbation of the tryptophans, the three common tryptophans, W161, W175, and W275 (W265 of bovine rhodopsin), are expected to interact with retinal. However, it is too early to conclude which tryptophan is changed during each transformation before we get octopus rhodopsin mutants like those in the case of bovine rhodopsin (Lin and Sakmar, 1996).

This work is supported in part by a grant from the Japanese Ministry of Education, Culture, Sports and Science.

## REFERENCES

- Bagley, K. A., L. Eisenstein, T. G. Ebrey, and M. Tsuda. 1989. A comparative study of the infrared difference spectra for octopus and bovine rhodopsins and their bathorhodopsin photointermediates. *Biochemistry*. 28:3366–3373.
- Cooper, A., S. F. Dixon, and M. Tsuda. 1986. Photoenergetic of octopus rhodopsin. *Eur. Biophys. J.* 13:195–201.
- Donovan, J. W. 1969. Physical Principles and Techniques of Protein Chemistry. S. J. Leach, editor. Academic Press, New York. 585–588.
- Ebrey, T. G. 1971. Energy transfer in rhodopsin, *n*-retinyl-opsin, and rod outer segments. *Proc. Natl. Acad. Sci. USA.* 68:713–716.
- Ebrey, T. G. 1972. The fluorescence from the tryptophan of rhodopsin. *Photochem. Photobiol.* 15:585–588.
- Farrens, D. L., and H. G. Khorana. 1995. Structure and function in rhodopsin. Measurement of the rate of metarhodopsin II decay by fluorescence spectroscopy. *J. Biol. Chem.* 270:5073–5076.
- Guzzo, A. V., and G. L. Pool. 1968. Visual pigment fluorescence. *Science*. 159:312–314.
- Guzzo, A. V., and G. L. Pool. 1969. Fluorescence spectra of the intermediates of rhodopsin bleaching. *Photochem. Photobiol.* 9:565–570.
- Hashimoto, S., H. Takeuchi, M. Nakagawa, and M. Tsuda. 1996. Ultraviolet resonance Raman evidence for the absence of tyrosinate in octopus rhodopsin and the participation of Trp residues in the transition to acid metarhodopsin. *FEBS Lett.* 398:239–242.
- Kitagawa, T., and M. Tsuda. 1980. Resonance Raman spectra of octopus acid and alkaline metarhodopsin. *Biochim. Biophys. Acta.* 624:211–217.
- Kusumi, A., S. Ohnishi, and M. Tsuda. 1980. Light-induced conformational change of octopus rhodopsin as detected by a spin label method. *Biochem. Biophys. Res. Commun.* 95:1635–1641.
- Kusumi, A., M. Tsuda, T. Akino, S. Ohnishi, and Y. Terayama. 1983. Protein-phospholipid-cholesterol interaction in the photolysis of invertebrate rhodopsin. *Biochemistry*. 22:1165–1170.
- Liang, J., G. Steinberg, N. Livnah, M. Sheves, T. G. Ebrey, and M. Tsuda. 1994. The pK<sub>a</sub> of the protonated Schiff bases of gecko cone and octopus visual pigments. *Biophys. J.* 67:848–854.
- Lin, S. W., and T. P. Sakmar. 1996. Specific tryptophan UV-absorbance changes are probes of the transition of rhodopsin to its active state. *Biochemistry*. 35:11149–11159.
- Masuda, S., E. Morita, M. Tasumi, T. Iwasa, and M. Tsuda. 1993a. Infrared studies of octopus rhodopsin: existence of a long-lived intermediate and the states of the carboxylic group of Asp81 in rhodopsin and its photoproducts. *FEBS Lett.* 317:223–227.
- Masuda, S., E. H. Morita, M. Tasumi, T. Iwasa, and M. Tsuda. 1993b. Infrared study of octopus rhodopsin and lumirhodopsin. *J. Mol. Struct.* 297:29–34.
- Ohtani, H., M. Kobayashi, M. Tsuda, and T. G. Ebrey. 1988. Primary processes in photolysis of octopus rhodopsin. *Biophys. J.* 53:17–24.
- Ovchinnikov, Y. A., N. G. Abdulaev, I. D. Artamonov, I. A. Beshpalov, A. E. Dergachev, and M. Tsuda. 1988. Octopus rhodopsin: amino acid sequence deduced from cDNA. *FEBS Lett.* 232:69–72.
- Pande, A. J., R. H. Callender, T. G. Ebrey, and M. Tsuda. 1984. Resonance Raman study of the primary photochemistry of visual pigments hypsorhodopsin. *Biophys. J.* 45:573–576.
- Pande, C., A. Pande, K. T. Yue, R. H. Callender, T. G. Ebrey, and M. Tsuda. 1987. Resonance Raman spectroscopy of octopus rhodopsin and its photoproducts. *Biochemistry*. 26:4941–4947.
- Sperling, W. 1973. Conformation of 11-*cis* retinal. In *Biochemistry and Physiology of Visual Pigments*. H. Langer, editor. Springer-Verlag, Berlin. 19–28.
- Stryer, L. 1986. Cyclic GMP cascade of vision. *Annu. Rev. Neurosci.* 9:87–119.

We thank Professor T. G. Ebrey, Center for Biophysics and Computational Biology, University of Illinois, and Dr. L. U. Colmenares, MSU-Iligan Institute of Technology, for useful discussions and critical reading of the manuscript. We are grateful to T. Fujinaka and K. Takahara for their technical assistance.



- Taiji, M., K. Bryl, M. Nakagawa, M. Tsuda, and T. Kobayashi. 1992. Femtosecond studies of primary photoproduct in octopus rhodopsin. *Photochem. Photobiol.* 56:1003-1011.
- Tokunaga, F., Y. Shichida, and T. Yoshizawa. 1975. A new intermediate between lumirhodopsin and metarhodopsin in squid. *FEBS Lett.* 55: 229-232.
- Tsuda, M. 1987. Photoreception and phototransduction in invertebrate photoreceptor. *Photochem. Photobiol.* 45:915-931.
- Tsuda, M. 1979. Transient spectra of intermediates in the photolytic sequence of octopus rhodopsin. *Biochim. Biophys. Acta.* 545:537-546.
- Tsuda, M., F. Tokunaga, T. G. Ebrey, K. T. Yue, J. Marque, and L. Eisenstein. 1980. Behavior of octopus rhodopsin and its photoproducts at very low temperatures. *Nature.* 287:461-462.
- Tsuda, M., T. Tsuda, and H. Hirata. 1989. Cyclic nucleotides and GTP analogues stimulate light-induced phosphorylation of octopus rhodopsin. *FEBS Lett.* 257:38-40.
- Tsuda, M., T. Tsuda, Y. Terayama, Y. Fukada, T. Akino, G. Yamanaka, L. Stryer, T. Katada, M. Ui, and T. G. Ebrey. 1986. Kinship of cephalopod photoreceptor G-protein with vertebrate transducin. *FEBS Lett.* 192: 5-10.